ADVANCED MATERIALS
www.advmat.de

Laser-Induced Molybdenum Carbide–Graphene Composites for 3D Foldable Paper Electronics

Xining Zang, Caiwei Shen, Yao Chu, Buxuan Li, Minsong Wei, Junwen Zhong, Mohan Sanghadasa, and Liwei Lin**

Versatile and low-cost manufacturing processes/materials are essential for the development of paper electronics. Here, a direct-write laser patterning process is developed to make conductive molybdenum carbide–graphene (MCG) composites directly on paper substrates. The hierarchically porous MCG structures are converted from fibrous paper soaked with the gelatin-mediated inks containing molybdenum ions. The resulting Mo_3C_2 and graphene composites are mechanically stable and electrochemically active for various potential applications, such as electrochemical ion detectors and gas sensors, energy harvesters, and supercapacitors. Experimentally, the electrical conductivity of the composite is resilient to mechanical deformation with less than 5% degradation after 750 cycles of 180° repeated folding tests. As such, the direct laser conversion of MCGs on papers can be applicable for paper-based electronics, including the 3D origami folding structures.

Disposable and flexible electronics have attracted great attentions in the past decade[1] while paper has been viewed as one key low-cost, environmentally friendly substrate[2] for various applications such as paper-based energy generators,[3,4] batteries,[5,6] supercapacitors,[7–10] sensors/actuators,[11] diagnosis devices,[12] and microfluidics systems.[13] In general, the functional components of such systems are deposited on paper using schemes such as wax printing,[14] evaporation,[15] and lithography.[16] Combined with origami techniques, paper electronics with deformable structures and 3D designs have been constructed[17] to assemble different components with high density.[18] Furthermore, the possibility of converting wasted papers to graphene has also been reported with the evaporation and annealing of Ag as contract pads.[15] However, these techniques generally utilize expensive equipment or expensive materials (noble metal such as Au and Ag), which increase the manufacturing cost. Here, we propose and demonstrate the direct laser patterning and conversion of ink-soaked paper substrates to multifunctional carbide–graphene composites to build the paper-based 3D foldable devices (an illustrating device in **Figure 1**a with the simplified conversion process in Figure 1b). Applications to mechanical energy harvesters, chemical sensors, and electrochemical supercapacitors are a few examples for paper-based electronics, we present demonstration results by using prototype devices in this work.

The laser writing and origami techniques for 3D foldable paper electronics are all carried out under ambient environment. Gelatin-mediated inks containing Mo^{5+} ions are first sprayed on paper substrates. As-prepared samples are then laser scanned (CO_2 laser by Tek Motion with wavelength of 10.6 μm) to convert paper substrates to hierarchically porous molybdenum carbide–graphene (MCG) composites. Optical photos and scanning electron microscopy (SEM) images of the original paper, paper soaked with gelatin ink, and the paper with converted MCG composites on the surface are compared (Figure S1, Supporting Information). With the optimized solution concentration, laser power and scan rate, the resulting MCG layer can reach an electrical resistance of 30 Ohm per square. The recovery of conductance after repeated mechanical bending and folding tests shows high mechanical stability for potential applications in 3D foldable paper electronics. For example, several square shape electrodes are fabricated on a single piece of paper (Figure 1c) and folded to make multiple supercapacitor cells to be connected in series or in parallel (inset in Figure 1c). In another example, the MCG on paper is proven to be resilient to repeated folding operations, while typical electrical connections using metals such as Ag in paper electronics are usually susceptible to failure under such deformation. Specifically, it is found that the first 50 folding test can generally induce a large change in conductivity (13% degradation in the prototype device). However, the conductivity can maintain its value with less than 5% decay in the following 750 cycles under the 180° folding tests in Figure 1d. It is believed that

Dr. X. Zang, C. Shen, B. Li, Dr. M. Wei, Dr. J. Zhong, Prof. L. Lin
Mechanical Engineering
University of California Berkley
Berkeley, CA 94704, USA
E-mail: xining.zang.me@berkeley.edu; lwlin@berkeley.edu
Dr. X. Zang, C. Shen, B. Li, Dr. M. Wei, Dr. J. Zhong, Prof. L. Lin
Berkeley Sensor and Actuator Center
Berkeley, CA 94704, USA
Y. Chu, Prof. L. Lin
Tsinghua Berkeley Shenzhen Institute
Shenzhen 518055, China
Dr. M. Sanghadasa
Aviation and Missile Research, Development, and Engineering Center
US Army
Redstone Arsenal, AL 35898, USA
The ORCID identification number(s) for the author(s) of this article can be found under https://doi.org/10.1002/adma.201800062.

DOI: 10.1002/adma.201800062

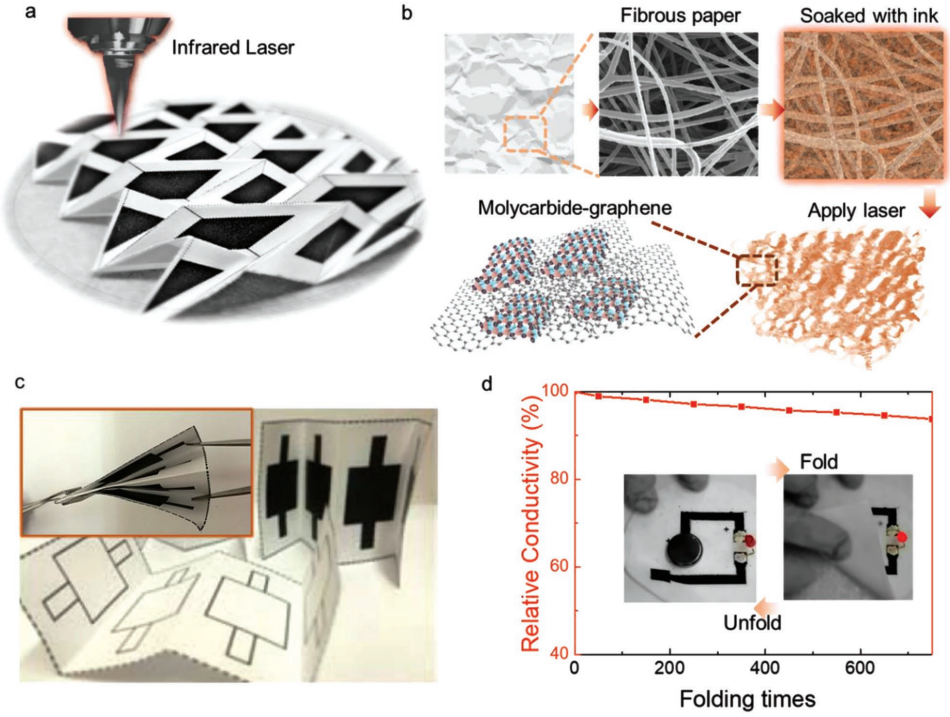

Figure 1. a) An optical photo of a fabricated origami structure after the direct laser-write MCG patterning process (black color areas) on a paper substrate (white color areas). b) Schematic illustration of the simplified MCG process from fibrous paper, soaked with the gelatin-mediated ink containing Mo^{5+} ions, laser conversion process, to the resulting MCG composites. c) Two partially folded, four 2×2 cm^2 electrodes on a paper substrate: (top) after the laser conversion process, and (bottom) before the conversion process. (inset) A fully folded device with two electrodes on top and two electrodes at the bottom for a two-capacitor in sandwich structure to be connected in series or parallel as supercapacitors. d) Recorded relative conductivity of an electrical connector made of MCG composites during the 750 cycles of 180° mechanical folding tests. (inset) Using mechanical folding and touching of electrodes made of MCG composites as an electrical switch to turn on/off a red light-emitting diode.

most of the permanent physical deformation occurred in the first 50 cycles (13% of resistance change) and there was only minor permanent physical deformation afterward in the next 750 cycles (less than 5% change). Using this feature, a simple electrical switch by mechanical folding/unfolding to make the contacts of two MCG electrode is realized (inset in Figure 1d) to turn on/off a light-emitting diode (LED).

The fabricated MCG structures are characterized by scanning electron microscopy (SEM), transmission electron microscopy (TEM), Raman spectroscopy, and X-ray diffraction (XRD). **Figure 2**a compares the microstructure of paper, paper soaked with ink, and after the laser conversion process, respectively, from the left, center, and right portion in the figure. The blank paper sample (a typical copy paper from Boise Aspen 30) has porous structures with fibers of 10–30 µm in diameter. After soaking with the Mo-gelatin ink, some large continuous regions of the gelatin ink are observed. The laser conversion process results in porous MCG structures with the enlarged view shown in Figure 2b, where various pore sizes ranging from hundreds of nanometers to several microns are observed. The TEM image of the converted MCG composites shows carbide particles with sizes down to ≈10 nm (Figure 2c). Raman and XRD results reveal the existence of both Mo_3C_2 and graphene after the conversion process in Figure 2d,e, respectively. The TEM images (Figure S2, Supporting Information) at the lower contrast color area show large sheet-shape structures and the atomic-fringe analyses indicate the interlayer distance of 3–4 Å which is consistent with the multiple-layer graphene formation instead of other carbon species. The Raman spectrum (Figure S5e, Supporting Information) also indicates that I_G/I_{2D} ratio is close to 1 which implies the material as graphene and the I_D value is small as compared to other carbonaceous structures such as amorphous carbon, carbon black, etc.[19–21] Furthermore, the D+D″ peak (two phonon intervalley scattering) and D+D′ (one phonon intravalley and one intervalley scattering) peak are observed implying defected graphene structures.[19] The Mo_3C_2 is the product of high-temperature carbonization of the Mo ions and gelatin and the presence of graphene is a synergistic result of laser annealing of paper and gelatin containing carbon atoms. The Mo-gelatin ink absorbs IR energy effectively to result in high local temperature to enable the gas phase reaction and "recrystallization" into the form of graphene.[22] On the other hand, the direct laser irradiation on a paper without the gelatin ink under similar laser power results in broken ashes as expected (Figure S3, Supporting Information). These results suggest that the Mo-gelatin ink solution can absorb and damp the laser energy to enable the formation of the MCG composites. In terms of the paper types, six different commercial papers have been tested and they have all shown successful conversions of the MCG composites, but they have resulted in different electrical resistances (Figure S4, Supporting Information). It is found that thick papers can absorb and hold more ink to achieve low sheet resistance after the laser conversion process. The commercial copy paper is found

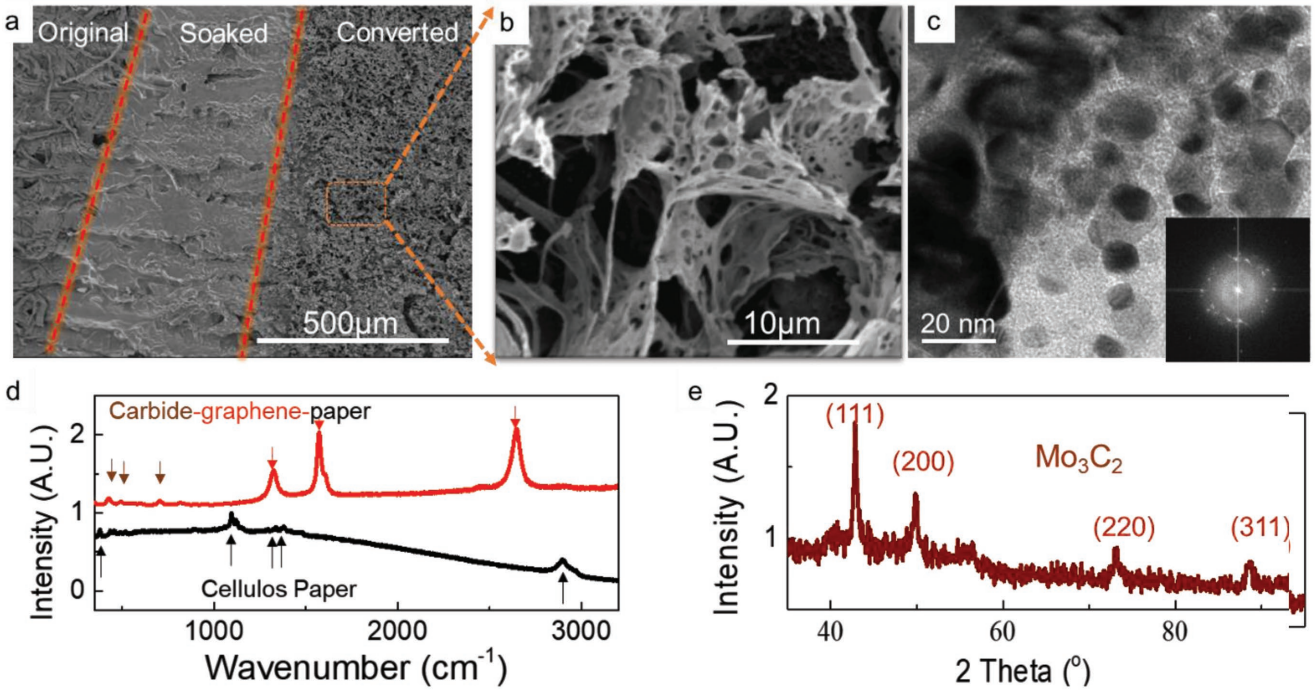

Figure 2. a) SEM image of a paper with three regions from left to right: paper, paper soaked with Mo-gelatin ink, and paper with converted MCG composites, respectively. b) Enlarged SEM view of the MCG composites showing porous structures. c) TEM image showing the Mo_3C_2 nanoparticles (dark color) and the background carbon-based materials. Inset: diffraction pattern analysis revealing the nanocrystalline Mo_3C_2 structures. d) Raman spectroscopy of the MCG sample showing the coexistence of graphene and molybdenum carbide, in comparison to the commercial cellulose paper. e) XRD analysis showing signature peaks of Mo_3C_2. Minor peaks are attributed to potential impurities in the commercial paper and the very rough surface which can introduce bumpiness in XRD.

to have both good mechanical strength and decent sheet resistance such that it is used throughout this work unless specified.

To optimize the conductivity of the MCG composites, the parameters of the laser writing process and the recipe of the Mo-gelatin ink are investigated. The SEM images and measured sheet resistance of the MCG composites under different laser power and scan rates are presented in **Figure 3**. In general, high laser power coupled with the low scanning rate can result in more energy inputs per unit area and this could lead to laser ablation and severe damages of the substrate in the extreme cases (such as 4 W, 250 mm s^{-1}). On the other hand, low laser power coupled with the high scanning rate can lead to less energy inputs per unit area without the successful MCG conversions. The SEM images of laser conversion result for laser power from 0.5 to 4 W under a fixed scanning speed of 250 mm s^{-1} and Mo ion concentration of 2 m, where m represents the mass molarity, are shown in Figure 3a–e. With a scan rate of 250 mm s^{-1}, 0.5 W of laser power cannot convert the ink-soaked paper to MCG composites as the sample remains mostly in the form of fabrics, while higher laser power below 3 W results in the MCG composites with high porosity. On the other hand, the SEM images of laser conversion results under a fixed laser power of 2 W with increasing scanning speed from 50 to 550 mm s^{-1} and Mo ion concentration of 2 m are shown in Figure 3f–j. In these figures, the porosity of the MCG composites reduces as the scanning speed increases. The sheet resistance for samples in Figures 3a–e is plotted in Figure 3k and a threshold power (≈2 W in this case) is found to be necessary to make the conductive MCG composites and further increase of the laser power does not seem to affect the conductivity. The sheet resistance results for samples in Figures 3f–j are plotted in Figure 3l. It is found that under a laser power of 2 W, the maximum threshold scan rate is 250 mm s^{-1} to make the conductive MCG composites. In this work, we choose 2 W and 250 mm s^{-1} as the standard process parameters to avoid potential damages to the paper substrate from higher laser energy.

The composition of the Mo ink, such as the type of hydrogel polymer, as well as the concentration of Mo ions, can also affect the property of the MCG composites. Different types of the water-soluble polymers, including gelatin, poly(ethylene oxide) (PEO), and poly(vinylpyrrolidone) (PVP) have been mixed with the Mo ions for tests. Conversion results show that 2 m Mo^{5+} solutions with PEO and PVP will result in very high sheet resistance of 15.8 and 7.56 MΩ per square, respectively (Figure S5d, Supporting Information), while gelatin-based ink can produce a much lower sheet resistance of 51.3 Ω per square. The usage of gelatin in the process is beneficial for two key reasons. 1) Gelatin can form triple helix structures to result in layer-by-layer lamellar morphology with embedded Mo^{5+} ions as discussed in a recently published paper.[23] This layer-by-layer structure increases the carbide and carbon network connections for improved conductivity. On the other hand, the laser conversion process of Mo-PEO and Mo-PVP inks results in the aggregated particle structures with nonuniform distributions and connections. 2) Gelatin is the combination of porcine skin peptides with rich amino acid functional groups that could bind strongly

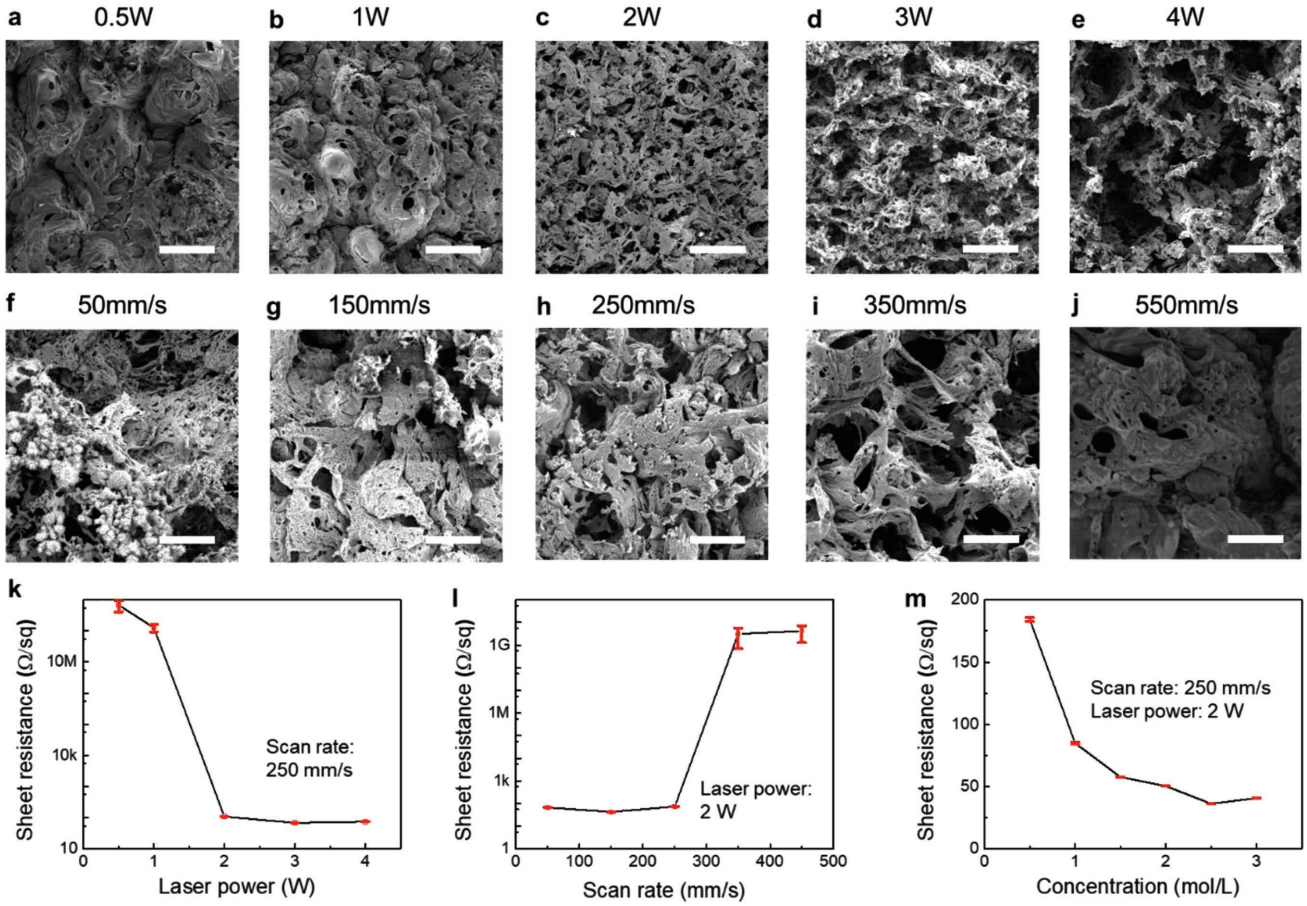

Figure 3. a–e) SEM images of MCG produced by various laser power from 0.5 to 4 W at a fixed scan rate of 250 mm s^{-1} and Mo ion concentration of 2 m. f–j) SEM images of MCG produced by various scan rates from 50 to 450 mm s^{-1} at a fixed power of 2 W and Mo ion concentration of 2 m. Scale bar = 100 µm for all images. k) Sheet resistance of the MCG sample produced by different laser power under a fixed scan rate of 250 mm s^{-1} and Mo ion concentration of 2 m. l) Sheet resistance of the MCG sample produced by different scan rate under a fix laser power of 2 W and Mo ion concentration of 2 m. m) Sheet resistance of the MCG samples produced by using inks with various Mo ion concentrations at a fixed power of 2 W and laser scan rate of 250 mm s^{-1}.

with Mo^{5+} ions to increase the absorption of the CO_2 laser at 10.6 µm (Figure S6, Supporting Information) to achieve higher local temperature. From the Raman Spectrum, optical images and SEM images (Figure S5a–c, Supporting Information), the conversion processes of Mo-PEO and Mo-PVP papers are not as effective for the conversions to graphene (Figure S5e,f, Supporting Information) and results in low electrical conductivity.

Gelatin-based inks with various Mo ion concentrations are also investigated. When the Mo ion concentration increases from 0.5 to 1 m, the sheet resistance can reduce by 50% (Figure 3m). Further increase of the Mo concentration can decrease the resistance gradually to reach a plateau when the Mo concentration is 2.5 m. The lowest sheet resistance is achieved as ≈Ω per square with 2 W of laser power, 250 mm s^{-1} scan rate, and gelatin ink with Mo^{5+} concentration of 2.5 m. Furthermore, inks with higher concentration of Mo ions show darker color when soaked in paper (Figure S7, Supporting Information), and the converted MCG composites show higher Mo signals under the electron dispersion spectrum tests (EDS, Figure S8, Supporting Information) which implies higher Mo_3C_2 loading. The conductivity values saturate when the Mo^{5+} concentration reaches 2 m and this concentration is used throughout this work. Higher Mo^{5+} concentration does not improve the conductivity, which could be attributed to two possible reasons: 1) high concentration ions result in the aggregated structure which can harm the uniform network; 2) high concentration ink might not be fully converted under the same IR energy (2 W) without further conductivity improvements. From the EDS spectrum of five samples using the 2 m Mo-gelatin ink, the molybdenum carbide concentration in the converted paper is 70.5 ± 8.5% (Figure S8, Supporting Information).

The laser converted MCGs are electrically conductive and mechanically stable such that they can be used as conductive layers such as electrodes or interconnectors in paper electronics, while the surface chemistry of the Mo_3C_2 nanostructure can enable potential sensing and electrochemical capabilities for the functional devices. Several prototypes are designed, fabricated, and tested to illustrate the possible applications in these areas. The first category is electrochemical sensors, including 1) a heavy metal ion (such as Cu^{2+}) detector (**Figure 4**a,b), and 2) a gas sensor (Figure 4c,d). For heavy metal detectors, the MCG

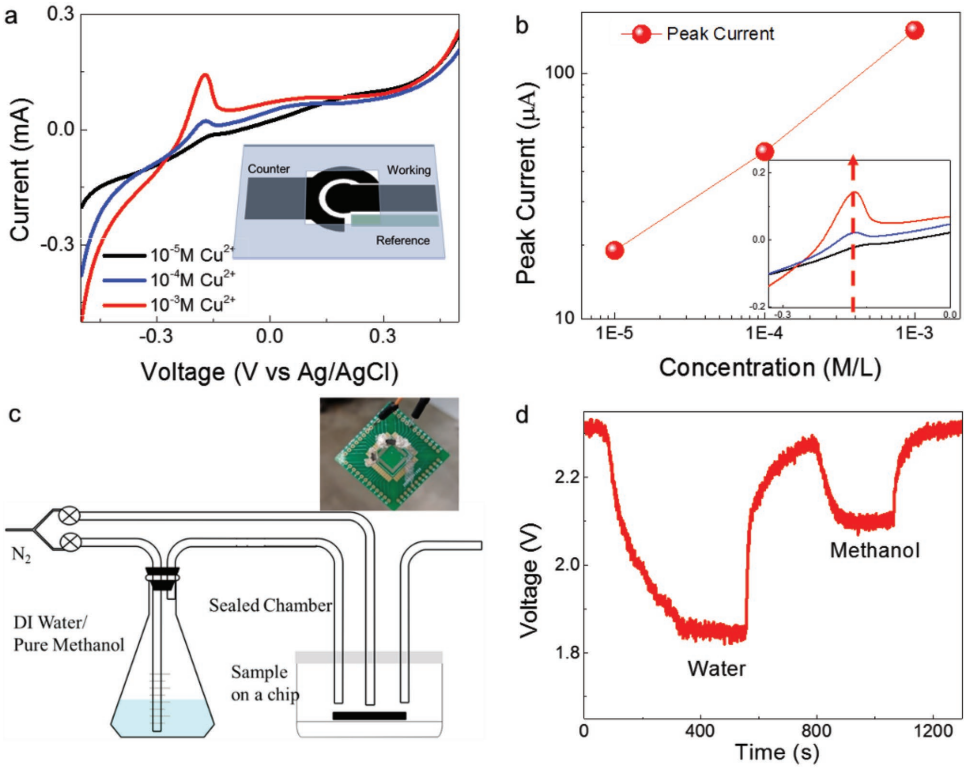

Figure 4. Paper-based electrochemical sensors made of laser converted MCG electrodes. a) The linear sweep voltammetry (LSV) curves from −0.5 to 0.5 V for the prototype paper-based Cu^{2+} detector with different Cu^{2+} concentrations from 10^{-5} to 10^{-3} M. (inset) Schematic of a three-electrode heavy metal ion detector using MCG as the counter and working electrodes and AgCl as the reference electrode. b) The peak current derived from the LSV curve versus the Cu^{2+} concentration. (inset) Enlarged view of the peaks on the LSV curves. c) Schematic of the gas sensing experimental setup and an optical photo showing the MCG-based gas sensor on a circuit board. d) Voltage versus time responses of the MCG gas sensor under a fixed current of 1 mA when saturated water and saturated methanol vapors are tested alternately.

composites are constructed as both the working (circular-shape electrode with tip diameter of 5 mm and width of 2 mm) and counter electrode (ring-shape electrode with inner diameter of 8 mm, outer diameter of 1 cm, and width of 2 mm) in a three-electrode system. The gap between the working and counter electrode is 2 mm and an Ag/AgCl electrode (rectangular electrode with width of 3 mm and length of 1 cm fabricated by the direct printing process) is used as the reference electrode. Experimental results show the distinguishable peaks in the linear sweep voltammetry (LSV) test with solutions containing 10^{-5}–10^{-3} M L^{-1} of Cu^{2+} (Figure 4a). In the 0.5 M H_2SO_4 media, the Cu^{2+} concentration of 10^{-5} M L^{-1} can be observed and the peak current versus Cu^{2+} concentration relationship is relatively linear as shown in Figure 4c. Furthermore, it is possible to achieve better resolution and sensitivity in the future work by using the linear stripping voltammetry method (instead of LSV) with a predeposition step to enrich the metal ions for better sensitivity.[24] For the MCG-based gas sensors, the porous MCG structure is potentially advantageous for large surface area-to-volume ratio for high sensitivity when the polarized gas molecules are absorbed to cause the doping effect on Mo_3C_2 and graphene. A gas sensing setup is shown in Figure 4c,d with preliminary testing results of the saturated water vapor and saturated methanol vapor at room temperature. The prototype sensor is made of MCG electrode with the size of 5 mm × 2 mm bonded by indium paste to a printed circuit board (PCB) board and the measured resistance of the MCG electrode decreases (voltage decreases under a constant current input) when saturated water or methanol vapor is applied and recovers to the original value under pure nitrogen. The measured sensitivity ($\Delta V/V$) is 11.9% and 2.4% for water and methanol, respectively, and the sensing mechanism is attributed to the physiosorbtion of gas doping effect for which electron is transferred to the valance band to increase the conductivity.[25]

In the second demonstration category, a paper-based piezoelectret generator is built[26] as illustrated in **Figure 5**a. The sandwich-like generator consists of three layers: the upper and bottom layers are electrodes made of MCG on paper; and the middle layer is a 100 μm thick, polytetrafluoroethylene (PTFE) film working as the electret material to keep the net charges following the previous work. By pressing and releasing the generator, the density of charges accumulated at both electrodes changes to induce an electrical current through the external circuit. It is found that a single paper-based generator can produce 150 V open-circuit voltage, and ≈11 μA of close-circuit current with an electrode area of 2.0 × 2.0 cm^2 in size. Inspired by the structure of origami fan and accordion, we also construct a parallel generator based on the fan structure as shown in Figure 5b, which has seven generators connected in parallel with electrodes of 2.0 × 2.0 cm^2 in size. The generator shows an open-circuit voltage of ≈150 V (Figure 5c) and a close-circuit current of ≈80 μA (Figure 5d). The prototype

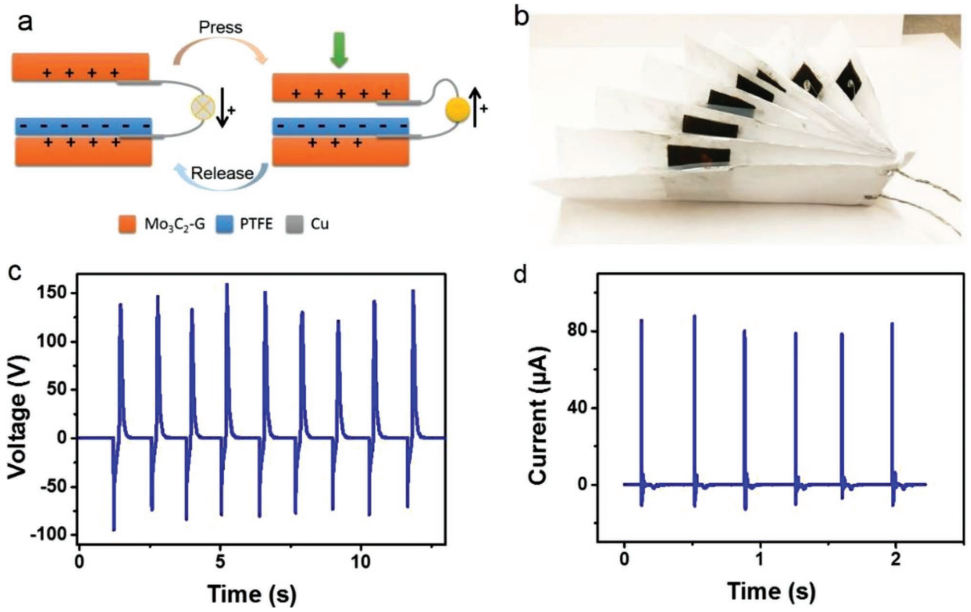

Figure 5. A paper-based piezoelectret generator made of laser converted MCG electrodes. a) Schematic of the components and working mechanism of the piezoelectret generator. b) An optical photo showing a paper-based piezoelectret generator based on the fan structure using seven generators connected in parallel. c) The open-circuit voltage and d) short-circuit current of the generator.

generator can provide power density up to ≈3 mW cm^{-2}, which could be further improved by optimizing the electret materials and increasing the device volume density using 3D foldable paper structures.[27] A second origami piezoelectret generator, in which the paper substrate with the Mo ink solutions is converted on both sides to achieve a "double folding" structure[28] is also fabricated and tested (Figure S9, Supporting Information).

In the third demonstration category, the supercapacitors via the paper-based MCG composites can be constructed with high surface areas to store energy based on the electrical double-layer effect and the reversible redox reactions.[25] The first design is based on interdigitated electrodes with three electrodes (1.5 mm in width and 8 mm in length) on each side and the gap between the electrodes is 0.2 mm (inset of **Figure 6**a). The electrode area is covered by electrolyte dried from the water solution of 1 M LiTFSI and 10 wt% PVA. Figure 6a shows the cyclic voltammetry (CV) curves of a single cell under various scan rates. The specific capacitances calculated are 14.0, 9.5, and 8.4 mF cm^{-2} from the CV curves with the scan rate of 1, 10, and 20 mV s^{-1}, respectively. These specific capacitance values are higher than those of supercapacitors with similar geometry made of direct-laser-write graphene on the polyimide tape (≈4 mF cm^{-2})[22] mainly due to the additional pseudocapacitance from Mo_3C_2. Figure 6b shows the capacitance retention results of a single cell after 11 000 cycles with no obvious change in the specific capacitance, indicating high stability of the electrodes. Devices with the 3D stacked and sandwich-structured cells can also be fabricated by laser patterning and assembled by folding paper substrates to achieve parallel connection, such as the design shown in Figure 1c. Figure 6c compares the CV curves of a single cell and two cells connected in parallel/series. Specific capacitances of 2.8, 5.3, and 1.7 mF cm^{-2} are achieved from the CV curves of the single cell, two stacked cells connected in parallel, and two stacked cells connected in series using a scan rate of 100 mV s^{-1}, respectively. Higher capacitance per unit area can be achieved by stacking of more cells, which is significant for applications having limited footprint area. As shown in Figure S10 (Supporting Information), the MCG-paper is hydrophilic which can improve the electrolyte–electrode contact. A single supercapacitor cell shows 296 Ohm series resistance, as shown in Figure S11 (Supporting Information). In this work, a supercapacitor with the design of interdigitated electrodes using four cells connected in series is used to power an LED as shown in Figure 6d as the demonstration toward a fully integrated system. Each cell is composed of in-plane interdigitated MCG electrodes directly patterned by laser. After charging the supercapacitor by 150 μA for 300 s, the system is able to power a 2.4 V LED for 10 s as shown.

In summary, the direct conversion and patterning of conductive and multifunctional MCG composites on the paper substrate has been achieved by using the CO_2 laser and gelatin-mediated Mo ion solutions. The converted hierarchically porous MCG structures have been characterized with the optimized electrical conductivity with respect to paper type, Mo ion concentration, laser power, and scan speed. The electrical testing results show that the MCG composites could be utilized as conductive electrodes for paper electronics, and three categories of device examples have been demonstrated: 1) porous electrodes for the electrochemical ion detectors and gas sensors; 2) 3D piezoelectret generators with the fan-structure; and 3) the energy storage systems such as supercapacitor electrodes. The multifunctional MCG composites produced by direct laser patterning could also lead to the integrated and self-sustained systems based on paper electronics. Specifically, a self-powered and self-sustained system could be intriguing, including sensors (such as the electrochemical sensors in Figure 4), energy harvesters (such as the piezoelectret generator in Figure 5), and energy storage devices (such as supercapacitor in Figure 6). These

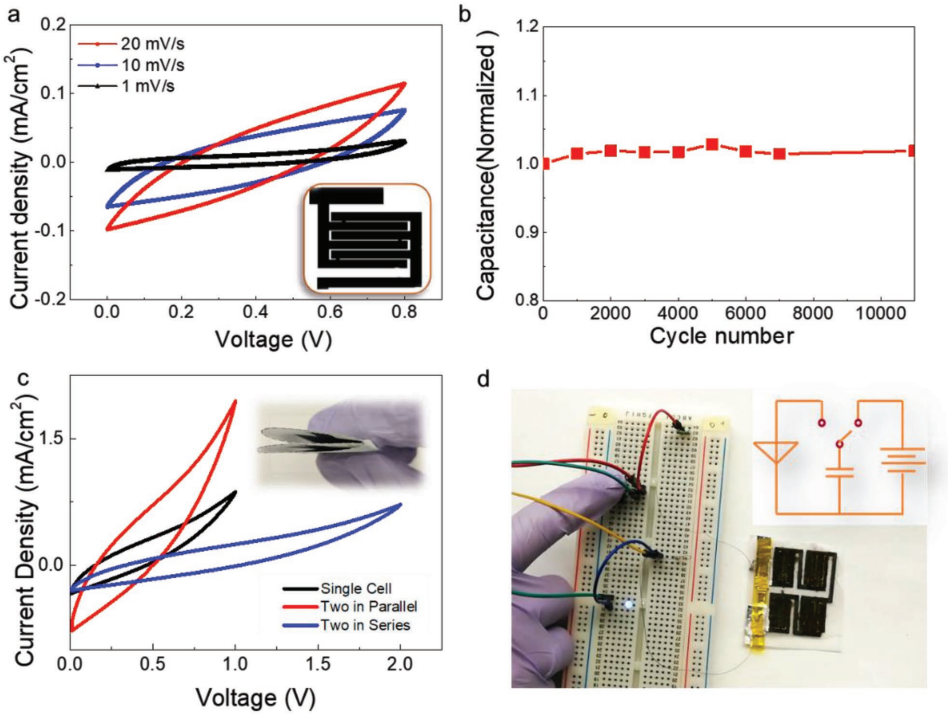

Figure 6. Paper-based supercapacitors using the MCG composites as electrodes. a) Measured CV curves of laser converted MCG composites for paper-based supercapacitors with the design of interdigitated electrodes and covered by the electrolyte dried from the water solution of 1 m LiTFSI and 10 wt% PVA. (Inset) Schematic of the supercapacitor cell with interdigitated electrode design. b) The capacitance retention results of a single cell in panel (a) during 11 000 cycles of charging and discharging operations. c) Measured CV curves of a single 3D sandwich-structure supercapacitor cell, a two-cell device connected in parallel, and a two-cell device connected in series. Scan Rate 100 mV s^{-1}. d) Optical photo of an interdigitated supercapacitor with four cells to power an LED.

could potentially promote practical applications in disposable and recyclable paper electronics.

Experimental Section

Gelatin-Mediated Mo Ion Ink Preparation: $MoCl_5$ (95 wt%, Sigma-Aldrich) was dissolved in deionized water, with different molar concentration: 1, 1.5, 2, 2.5, and 3 m with 60 wt% gelatin (powder, from porcine skin, type A, Sigma-Aldrich) heated to 60 °C to make homodispersed hydrogel ink.

Laser Converted MCG Composites on Paper: Mo-gelatin hydrogel was sprayed on different paper substrates (copy paper is the main substrate and other papers are compared in the Supporting Information). Paper soaked with the hydrogel ink was patterned by a CO_2 laser with different power varying from 0.5 to 4.0 W, and scan speed from 50 to 550 mm s^{-1}.

Characterization of MCG Composites: As patterned electrodes were tailored to 2 cm × 1 cm size to measure the sheet resistance (Keithley 2400). SEM (Quanta FEI) was used to characterize the structure of fabric paper and ablated paper with hierarchically porous structures. XRD (Bruker 8) and energy dispersive spectroscopy (EDS) were employed to verify the component and composition of MCG. Raman spectroscope (Renishaw inVia) was employed to study the composition and quality of as-converted graphene.

Applications of MCG in Paper-Based Electronics:

a) Piezoelectret generator: As-patterned MCG on paper is directly used as a conductor, which enables circuits to work even after repeated mechanical folding operations. To make a piezoelectret generator,[26] the MCG paper electrode is assembled with a piece of precharged PTFE thin film.
b) Electrochemical ion detectors and gas sensors: Three electrodes system on paper is made of two prepatterned MCG electrodes and one Ag/AgCl electrode besides, which is tested in 0.5 M H_2SO_4 media with different concentration of Cu^{2+}. The MCG electrodes on paper with hierarchically porous structure are also tested as a gas sensor, which is sensitive to the polarized molecules such as moisture and methanol.
c) Supercapacitors: Four pads with area of 2 × 2 cm^2 are patterned on one piece of paper, which is assembled and connected with aluminum wires to make supercapacitors connected in parallel or in series. Electrolytes made of PVA-LiTFSI (10% 1 m) are deposited onto the electrodes before the assembly and they also function as the separators. The electrochemical characterizations, including CV tests, are performed by a Gamry workstation.

Supporting Information

Supporting Information is available from the Wiley Online Library or from the author.

Acknowledgements

X.Z. and C.S. contributed equally to this work. This work was performed in part at the Molecular Foundry, a User Facility supported by the Office of Science, Office of Basic Energy Sciences, of the U.S. Department of Energy under Contract No. DE-AC02-05CH11231 and supported in part by the Berkeley Sensor and Actuator Center, an NSF/Industry/University Research Collaboration Center.

Conflict of Interest

The authors declare no conflict of interest.

Keywords

lasers, molybdenum carbides, paper electronics, sensors, supercapacitors

Received: January 3, 2018
Revised: February 17, 2018
Published online: May 15, 2018

[1] Y. H. Jung, T. H. Chang, H. L. Zhang, C. H. Yao, Q. F. Zheng, V. W. Yang, H. Y. Mi, M. Kim, S. J. Cho, D. W. Park, H. Jiang, J. Lee, Y. J. Qiu, W. D. Zhou, Z. Y. Cai, S. Q. Gong, Z. Q. Ma, *Nat. Commun.* **2015**, *6*, 7170.
[2] A. Russo, B. Y. Ahn, J. J. Adams, E. B. Duoss, J. T. Bernhard, J. A. Lewis, *Adv. Mater.* **2011**, *23*, 3426.
[3] Z. L. Wang, *ACS Nano* **2013**, *7*, 9533.
[4] Z. L. Wang, *Mater. Today* **2017**, *20*, 74.
[5] T. H. Nguyen, A. Fraiwan, S. Choi, *Biosens. Bioelectron.* **2014**, *54*, 640.
[6] Q. C. Liu, L. Li, J. J. Xu, Z. W. Chang, D. Xu, Y. B. Yin, X. Y. Yang, T. Liu, Y. S. Jiang, J. M. Yan, X. B. Zhang, *Adv. Mater.* **2015**, *27*, 8095.
[7] L. Nyholm, G. Nystrom, A. Mihranyan, M. Stromme, *Adv. Mater.* **2011**, *23*, 3751.
[8] V. L. Pushparaj, M. M. Shaijumon, A. Kumar, S. Murugesan, L. Ci, R. Vajtai, R. J. Linhardt, O. Nalamasu, P. M. Ajayan, *Proc. Natl. Acad. Sci. USA* **2007**, *104*, 13574.
[9] D. W. Wang, F. Li, J. P. Zhao, W. C. Ren, Z. G. Chen, J. Tan, Z. S. Wu, I. Gentle, G. Q. Lu, H. M. Cheng, *ACS Nano* **2009**, *3*, 1745.
[10] Y. Ko, M. Kwon, W. K. Bae, B. Lee, S. W. Lee, J. Cho, *Nat. Commun.* **2017**, *8*, 536.
[11] G. Grauy, E. J. Frazier, V. Subramanian, *Microsyst. Nanoeng.* **2016**, *2*, 16032.
[12] A. A. Kumar, J. W. Hennek, B. S. Smith, S. Kumar, P. Beattie, S. Jain, J. P. Rolland, T. P. Stossel, C. Chunda-Liyoka, G. M. Whitesides, *Angew. Chem., Int. Ed.* **2015**, *54*, 5835.
[13] A. W. Martinez, S. T. Phillips, G. M. Whitesides, E. Carrilho, *Anal. Chem.* **2010**, *82*, 3.
[14] E. Carrilho, A. W. Martinez, G. M. Whitesides, *Anal. Chem.* **2009**, *81*, 7091.
[15] D. Tobjork, R. Osterbacka, *Adv. Mater.* **2011**, *23*, 1935.
[16] J. A. Rogers, Z. Bao, K. Baldwin, A. Dodabalapur, B. Crone, V. R. Raju, V. Kuck, H. Katz, K. Amundson, J. Ewing, P. Drzaic, *Proc. Natl. Acad. Sci. USA* **2001**, *98*, 4835.
[17] P. K. Yang, Z. H. Lin, K. C. Pradel, L. Lin, X. H. Li, X. N. Wen, J. H. He, Z. L. Wang, *ACS Nano* **2015**, *9*, 901.
[18] S. Felton, M. Tolley, E. Demaine, D. Rus, R. Wood, *Science* **2014**, *345*, 644.
[19] A. C. Ferrari, D. M. Basko, *Nat. Nanotechnol.* **2013**, *8*, 235.
[20] A. C. Ferrari, J. Robertson, *Philos. Trans. R. Soc., A* **2004**, *362*, 2477.
[21] P. K. Chu, L. H. Li, *Mater. Chem. Phys.* **2006**, *96*, 253.
[22] J. Lin, Z. W. Peng, Y. Y. Liu, F. Ruiz-Zepeda, R. Q. Ye, E. L. G. Samuel, M. J. Yacaman, B. I. Yakobson, J. M. Tour, *Nat. Commun.* **2014**, *5*, 5714.
[23] H. Jang, B. Seong, X. Zang, H. Lee, J. W. Bae, D. Cho, E. Kao, C. Yang, G. Kang, Y. Liu, H. S. Park, D. Byun, L. Lin, *Adv. Mater. Interfaces* **2018**, *5*, 1701491.
[24] W. Gao, H. Y. Y. Nyein, Z. Shahpar, H. M. Fahad, K. Chen, S. Emaminejad, Y. J. Gao, L. C. Tai, H. Ota, E. Wu, J. Bullock, Y. P. Zeng, D. H. Lien, A. Javey, *ACS Sen.* **2016**, *1*, 866.
[25] B. Li, Y. Chu, X. Zang, M. Wei, H. Liu, Y. Liu, Y. Ma, C. Li, X. Wang, L. Lin, *2017 19th Int. Conf. Solid-State Sensors, Actuators and Microsystems (TRANSDUCERS)*, IEEE, Piscataway, NJ, USA **2017**, p. 335, https://doi.org/10.1109/TRANSDUCERS.2017.7994056.
[26] J. W. Zhong, Q. Z. Zhong, X. N. Zang, N. Wu, W. B. Li, Y. Chu, L. W. Lin, *Nano Energy* **2017**, *37*, 268.
[27] T. B. H. Schroeder, A. Guha, A. Lamoureux, G. vanRenterghem, D. Sept, M. Shtein, J. Yang, M. Mayer, *Nature* **2017**, *552*, 214.
[28] S. L. Li, *Front. Optoelectron.* **2017**, *10*, 38.

